

We are IntechOpen, the world's leading publisher of Open Access books Built by scientists, for scientists

4,800

Open access books available

122,000

International authors and editors

135M

Downloads

Our authors are among the

154

Countries delivered to

TOP 1%

most cited scientists

12.2%

Contributors from top 500 universities



WEB OF SCIENCE™

Selection of our books indexed in the Book Citation Index
in Web of Science™ Core Collection (BKCI)

Interested in publishing with us?
Contact book.department@intechopen.com

Numbers displayed above are based on latest data collected.

For more information visit www.intechopen.com



Ammonia as a Hydrogen Source for Fuel Cells: A Review

Denver Cheddie

Additional information is available at the end of the chapter

<http://dx.doi.org/10.5772/47759>

1. Introduction

The concept of a hydrogen economy was revived in the 1990s as interest in fuel cell technology surged. There was an explosion of research into fuel cells since then mainly because of its status as a hydrogen technology, and as such both concepts shared a symbiotic relationship. However there are a number of problems with the direct use of hydrogen in fuel cells. Firstly hydrogen does not exist naturally. Secondly it is not easy to store or transport because of its low volumetric energy density and its small molecular size.

Recently the concept of an ammonia economy has gained eminence [1]. Like hydrogen, ammonia is carbon free and can be produced from any energy resource. However there are also some significant advantages in terms of storage and transport. Ammonia can be liquefied at room temperature at pressures of 8-10 bar and stored in a similar manner to propane, whereas hydrogen requires expensive cryogenic storage. In addition, ammonia allows for safer handling and distribution than hydrogen. Although it is toxic, its smell can be detected even at safe concentration levels (< 1 ppm). Ammonia has a narrower flammable range than hydrogen and is actually considered nonflammable when being transported, whereas hydrogen burns with an invisible flame. Ammonia is the second most widely produced commodity chemical in the world (second to sulfuric acid), with over 100 million tons per year being transported [2], and as such its worldwide distribution system is well established. Such is not the case for hydrogen. In fact, one major drawback with hydrogen technologies is the fact that the necessary hydrogen infrastructure does not presently exist. Essentially the ammonia economy can achieve the same benefits of a hydrogen economy, but using infrastructure that already exists.

Ammonia provides a source of hydrogen for fuel cells. It contains 17% hydrogen by weight, which can be extracted via thermal catalytic decomposition or electro-oxidation. Alternatively ammonia may be oxidized directly in fuel cells without the need for a separate

reactor. Table 1 compares the storage capabilities of various fuels based on their higher heating value (HHV) [3]. Hydrogen has a very low energy density (per volume) because of its low density. Ammonia's energy density is comparable to that of compressed natural gas (CNG) and methanol, but lower than gasoline and liquefied propane gas (LPG). Per unit volume, the cost of hydrogen energy is lower than that of ammonia energy, but hydrogen has less energy stored per volume than ammonia. Per unit energy, ammonia is the cheapest energy source listed in Table 1 – estimated at US\$13.3/GJ. Note that these values are based on the HHV of the fuel and do not account for conversion of this energy to useful forms. The life cycle production cost of energy from ammonia is estimated at US\$1.2/kWh compared to US\$3.8/kWh for methanol and US\$25.4/kWh for hydrogen [4]. Thus ammonia presents a very viable and cost effective fuel for fuel cells.

This chapter reviews the progress of ammonia fuel cells – those that use ammonia directly or indirectly. Ammonia fuel cells have been previously reviewed [5-7]. Ref [5] was published in 2004 and provides a mini-review focusing only on decomposition catalysts. Ref [6] was published in 2008 and provides a good review up to that point, however it only addresses decomposition catalysts, ammonia fed SOFCs and SOFC modeling. Ref [7] was published more recently (2011) but gave a more general overview rather than integrate research findings in the different areas of research in ammonia fuel cells. The present work seeks to integrate the research findings and provide a wide picture of the research conducted in ammonia fuel cells, and to show the development of the field. It also highlights areas that warrant further investigation to fully develop the field. Section 2 discusses developments in hydrogen generation for fuel cells via thermal decomposition of ammonia, electro-oxidation of ammonia, and from ammonia products. Section 3 outlines the development of direct ammonia fuel cells, citing experimental studies and their results. Section 4 reviews the various works done on mathematical modeling and simulation of ammonia fuel cells.

Fuel / Storage System	P (bar)	Energy Density (GJ/m ³)	Specific Volumetric cost (US\$/m ³)	Specific Energy Cost (US\$/GJ)
Ammonia gas / pressurized tank	10	13.6	181	13.3
Hydrogen / metal hydride	14	3.6	125	35.2
Gasoline (C ₈ H ₁₈) / liquid tank	1	34.4	1000	29.1
LPG (C ₃ H ₈) / pressurized tank	14	19.0	542	28.5
CNG (CH ₄) / integrated storage system	250	10.4	400	38.3
Methanol (CH ₃ OH) / liquid tank	1	11.4	693	60.9

Table 1. Energy Storage Capabilities of Various Fuels [3]

2. Hydrogen generation from ammonia

Hydrogen can be produced from ammonia for use in fuel cells in various ways. Most of the literature is devoted to thermal decomposition or catalytic cracking of ammonia into

nitrogen and hydrogen, with fewer articles addressing electrolysis or electro-oxidation. Some papers also address hydrolysis of ammonia products such as ammonia borane.

2.1. Catalytic decomposition of ammonia



Ammonia is unstable at high temperatures and begins to decompose at 200 °C [7]. The slightly endothermic decomposition reaction is shown in equation 1. Thermodynamically, 98-99% conversion of ammonia to hydrogen is possible at temperatures as low as 425 °C. However in practice, the rate of conversion depends on temperature as well as catalysts.

Thermal decomposition or catalytic cracking is the most common means of hydrogen generation from ammonia. Lipman and Shah [8] report that for large scale hydrogen generation (> 1000 m³/hour), reformation of natural gas remains the most cost effective process, however for small scale generation, (< 10 m³/hour), ammonia cracking becomes slightly more economical than natural gas reformation (see Table 2). This study is based on lifecycle cost analysis, taking into account investment and operation costs.

Scale of H ₂ production (m ³ /hour)	Cost of H ₂ production, US\$ / (m ³ /hour)			
	Water Electrolysis	Natural Gas Reformation	Methanol Reformation	Ammonia Cracking
10	0.943	0.390	0.380	0.343
100	0.814	0.261	0.285	0.279
1000	0.739	0.186	0.226	0.241

Table 2. Life Cycle Cost of Hydrogen Production via Various Processes [8]

The early studies done on ammonia decomposition focused more on ammonia synthesis, and as such considered iron based catalysts. Since then various metals, alloys, and compounds of noble metal characters have been tested for ammonia decomposition. These include Fe, Ni, Pt, Ru, Ir, Pd, Rh; alloys such as Ni/Pt, Ni/Ru, Pd/Pt/Ru/La; and alloys of Fe with other metal oxides including Ce, Al, Si, Sr, and Zr [5]. Various catalysts have been investigated for decomposing ammonia to produce hydrogen for alkaline fuel cells. These include WC, Ni/Al₂O₃, NiCeO₂/Al₂O₃, Cr₂O₃, Ru/ZrO₂, and Ru on carbon nano-fibres. Caesium-promoted ruthenium supported on graphite was also found to be very promising [7]. For these catalysts, a minimum temperature of 300 °C is required for efficient release of ammonia for hydrogen production.

The performance of the catalysts can be quantified using the rate of hydrogen production, conversion fraction of ammonia (fraction of ammonia that is converted to hydrogen), and activation energy. The rate of formation of hydrogen from ammonia decomposition has been measured experimentally, typically in units of millimoles of hydrogen produced per minute per gram of catalyst loaded (mmol/min/g). The performance of various catalysts for ammonia decomposition, reviewed in this section, is summarized in Table 3.

Catalyst / Support	Temp. (°C)	Rate of H ₂ Gen. (mmol/min/g)	Conv. Eff. (%)	Ref.
Nano-sized Ni/Santa Barbara Amorphous (SBA)-15 support	450	8.4	25.0	[11]
	500	17.4	52.1	
	550	26.8	80.1	
	600	31.9	95.2	
	650	33.2	99.2	
Ni/SBA-15	550	12.7	37.8	[12]
Ni/SiO ₂	400	0.4	1.4	[10]
	500	3.3	10.5	
	550	6.8	21.6	
	600	11.4	36.4	
	650	21.1	70.0	
Ni/SiO ₂	550	11.6	34.6	[12]
Ni/Al ₂ O ₃	550	12.7	37.8	[13]
Ni/Al ₂ O ₃	500	24.1	71.9	[14]
Ni/Al ₂ O ₃ coated cordierite monolith Ni/Al ₂ O ₃ (unsupported particles < 200 μm)	550	16.5	50.0	[15]
		13.2	40.0	
Ir/SiO ₂	400	1.2	3.9	[10]
	500	5.7	18.2	
	600	17.6	56.0	
	700	30.6	98.0	
Ru/SiO ₂	400	4.5	14.3	[10]
	500	20.0	64	
	600	30.3	97	
	650	30.9	99	
Ru/ZrO ₂	550	25.8	77.0	[16]
Ru/Al ₂ O ₃		23.5	73.7	
Ru/CNT	400	6.2	3.7	[16] ^a
Ru/K-CNT		12.2	7.3	
Ru/K-ZrO ₂ -BD		8.5	5.3	
Ru/ZrO ₂		3.7	2.2	
Ru/Al ₂ O ₃		3.8	2.3	
Ru/MgO		5.4	3.2	
Ru/TiO ₂		4.3	2.6	
Ru/CNT	400	6.0	9.0	[17] ^b
Ru/MgO-CNT		8.7	13.0	
Ru/CNT treated with KNO ₃	400	33.3	49.7	[18] ^b
Ru/CNT treated with KOH		31.6	47.2	
Ru/CNT treated with K ₂ CO ₃		31.3	46.7	

All studies are based on an ammonia gas hourly space velocity (GHSV) of 30,000 ml/h/g of catalyst except (a) GHSV = 150,000 ml/h/g and (b) GHSV = 60,000 ml/h/g.

Table 3. Summary of Ammonia Decomposition Catalysts Performance Reported

Papapolymerou and Bontozoglou [9] studied the rate of decomposition at 225 – 925 °C and 133 kPa ammonia partial pressure. They used the catalyst in the form of polycrystalline wires of foils, and ranked them in decreasing order of reaction rate: Ir > Rh > Pt > Pd. Choudhary et al [10] performed similar studies at 400 – 700 °C with pure ammonia and ranked them: Ru > Ir > Ni. Comparing Ni, Ir and Ru supported in silica, Ru based catalysts have been reported to produce the highest decomposition rates as well as the highest conversion rate of ammonia. Yin et al [5] studied the effect of Ru loading within the silica support (in the range 0-35 wt.%) and found that the conversion rate of ammonia reached a peak at 15% weight loading of Ru. It increased with Ru loading from 0-15%, but above this, the sublayers of Ru were inaccessible thus rendering them redundant.

Different supports have also been investigated. The purpose of the support is to enhance the dispersion and increase the effective area of the active catalyst. The support should be stable under reaction conditions and have a high specific surface area. For Ru catalyst, the various supports include silica, alumina, graphitized carbon, carbon nanotubes, and nitrogen doped carbon nanotubes [10,19-25]. Yin et al [16] ranked the supports for Ru in order of decreasing activity measured by ammonia conversion rate: Carbon nanotube (CNT) > MgO > TiO₂ > Al₂O₃ > ZrO₂ > AC > ZrO₂/BD. It was proposed that CNTs performed the best because they allowed the best dispersion of Ru and also because of their high purity. CNTs have the added advantage of high conductivity which aids in electron transfer thus facilitating the recombinative nitrogen desorption step (see section 2.2). They further showed that using a MgO-CNT support resulted in better performance of the Ru catalyst than using a MgO base or CNT base alone [17]. Temperature programmed hydrogenation results showed that MgO resulted in even greater stability for the CNT.

Studies have shown that acidic conditions are not suitable for ammonia decomposition. Yin et al [16] prepared CNT with KOH and found that they resulted in better catalytic performance measured by reaction rate and conversion efficiency. N₂-temperature programmed desorption (TPD) results showed that the stronger the basicity, the better the catalyst performance [16]. They later studied the effects of promoter cations and the amount of potassium on the morphological structure and catalysis of Ru/CNT [18]. Essentially they found that ammonia conversion increased as the electro-negativity of the promoter decreased. When Ru/CNT is treated with potassium nitrate, potassium hydroxide or potassium carbonate, the conversion rate of ammonia and the rate of hydrogen evolution are significantly improved (see Table 3). Yin et al [5] concluded that the best catalyst for ammonia decomposition is Ru supported on alkaline promoted CNT.

The problem with Ru is that it is a noble metal which will significantly increase the cost of the fuel cell system. For mass production, it is preferable to use less expensive materials. Ru is widely accepted as the most active catalyst for ammonia decomposition, however the performance of Ni is very close [26]. It is possible to substitute the noble catalyst by other more economic active phases. Plana et al [15] studied the effect of having the catalyst in the form of a structured reactor with the hope of extracting greater activity from less expensive metals. The small scales of microstructured devices have inherent advantages, including high heat and

mass transfer coefficients and high surface area to volume ratios. They considered cordierite monoliths, which are structured reactors with multiple channels of several hundreds of microns in diameter. Monoliths have uniform flow distribution and low pressure drop which is crucial for the energy-efficiency of the process. Furthermore, they are commercially available, and they can withstand high temperatures and their coating with catalyst layer is a mature technology [27]. They used coated cordierite monoliths with mesoporous alumina, on which they dispersed Ni by electrostatic adsorption. This catalytic structured reactor was thoroughly characterized by transmission electron microscopy (TEM), X-ray diffraction (XRD), N_2 physisorption and temperature programmed reduction (TPR), and it was tested in NH_3 decomposition for in situ H_2 generation under realistic conditions such as pure NH_3 feed and high space velocity. The structured catalyst reactor consisted of Ni supported on alumina-coated monoliths. After prolonged reaction, Ni remained well dispersed with particle sizes of 6 nm and mesopores between 4-5 nm. Ni remained anchored within the alumina matrix and did not plug the pores. 100% conversion of ammonia was observed at 600 °C. They found that at temperatures exceeding 500 °C, the monolith reactors showed better performance than a packed bed catalyst – higher conversion of ammonia and more robustness.

Table 3 shows that the best ammonia conversion and hydrogen generation rates via thermal decomposition are obtained using Ru/CNT catalysts treated with potassium based alkalis. Ni produces very good results as well but requires higher temperatures (500 – 600 °C) to produce equivalent performance of Ru at 400 °C. The advantage of Ni is that it is less expensive than Ru and can be loaded at high concentrations to achieve the desired results. An anode supported SOFC (with an anode thickness of 500 μm , 40% porosity and 50% Ni by volume) requires a Ni loading of 0.134 g/cm². If it is operated at a current density of 5000 mA/cm², it consumes hydrogen at the rate of 11.6 mmol/min/g of catalyst. If the cell operates at 600 °C, then Ni can safely decompose ammonia at the required rate.

2.2. Reaction mechanism of ammonia decomposition

Various studies have investigated the reaction mechanism of ammonia decomposition. The reaction steps include 1) adsorption of ammonia onto catalyst sites, 2) cleavage of N-H bond on adsorbed ammonia, 3) recombinative desorption of N_2 atoms [28]. These three steps are respectively illustrated in equations 2-4, where * refers to an active site and X^* refers to species X adsorbed onto an active site.



Early studies observed that the rate of ammonia decomposition over Pt and Fe, shifted from zero order with respect to ammonia partial pressure at low temperatures (< 500 °C) to first order at high temperatures [29]. Tsai and Weinberg [27] proposed that on Ru crystal

catalysts, below approximately 400 °C the recombinative desorption of nitrogen atoms (step 3) is rate limiting, whereas above 400 °C the cleavage of the N–H bond of adsorbed NH₃ (step 2) is rate limiting. This was based on the observation that the apparent activation energy decreased from 180 kJ/mol at the low temperatures to 21 kJ/mol at high temperatures. It should be noted however, that these early studies did not consider the effects of hydrogen inhibition.

Later studies observed that at low temperatures and low ammonia partial pressures, the released hydrogen acted as an inhibitor to the decomposition reaction. Bradford et al [19] sought to gain information on H₂ inhibition on NH₃ decomposition over Ru/C catalyst. NH₃ partial pressure was varied from 1.3–12.0 kPa with temperatures between 370–390 °C, and a first order dependence of the reaction rate on NH₃ was observed. They proposed the following equation where α varies from 0.69 to 0.75, and β varies from -1.5 to -2, while the activation energy was 96.6 kJ/mol.

$$r_{H_2} = k p_{NH_3}^{\alpha} p_{H_2}^{\beta} \quad (5)$$

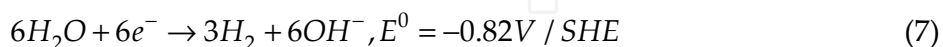
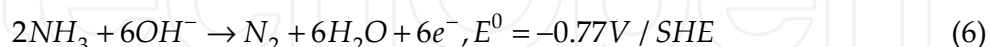
Egawa et al [30] used deuterated NH₃ on Ru single crystal surfaces and determined that the inhibition by H₂ was a consequence of an equilibrium established among adsorbed nitrogen atoms, gas-phase NH₃, and gas-phase H₂; and that recombinative desorption of adsorbed nitrogen atoms was the rate determining step. Vitvitskii et al [31] came to a similar conclusion based on experimental results acquired with diluted NH₃. Boudart et al [28] proposed that over W and Mo catalysts, N-H bond cleavage and recombinative desorption of surface nitrogen atoms are slow irreversible steps in NH₃ decomposition, NH₃ is activated via a direct dissociative adsorption step, and the adsorbed N atoms are the most abundant reactive intermediate.

Skodra et al [32] found that at higher temperatures (350 – 650 °C) and low ammonia partial pressures (0.5 – 2.0 kPa) over a Ru catalyst, hydrogen inhibition was no longer significant. They also observed a second order dependence of the rate of decomposition on ammonia partial pressure. This was explained by assuming step 3 above was the rate determining step. Shustorovich and Bell [33] suggested, based on the BOC Morse potential method, that the rate-determining step of ammonia decomposition is recombinative desorption of N₂. Chellappa et al [34] investigated pure ammonia (high concentration) over Ni-Pt/Al₂O₃ catalyst at 520 – 690 °C, and H₂ inhibition was not observed. The reaction was first order with respect to NH₃ pressure, and the activation energy was 196.2 kJ/mol.

Thus it appears that H₂ inhibition is only significant at low NH₃ concentrations and low temperatures [5]. Earlier studies reported a shift in reaction order from 0 to 1 with respect to ammonia partial pressure as temperature increases, however more recent studies report a shift in reaction order from 1 to 2 with temperature. β varies between -1.5 and -2 at low temperatures and low ammonia concentrations, but shifts to 0 as temperature and ammonia concentration increase. There also appears to be a consensus among researchers that the recombinative desorption of nitrogen atoms is the rate determining step in the decomposition reaction.

2.3. Electrolysis of Ammonia

Electrolysis or electro-oxidation is another method of extracting hydrogen from ammonia. It has the advantage of scalability and versatility to interface with renewable energy sources including those whose electricity production varies with time [35]. Hydrogen can also be produced at moderate temperatures. It was first discussed by Vitse et al [35], who proposed the coupling of ammonia oxidation in an alkaline medium at the anode with the reduction of water at the cathode.



The thermodynamic potential for ammonia electrolysis in alkaline media is -0.77 V compared with -1.223 V for the electrolysis of water. The theoretical thermodynamic energy consumption is 1.55 Wh/g of H₂ from electrolysis of NH₃ compared to 33 Wh/g of H₂ from H₂O [36]. This means that theoretically, ammonia electrolysis consumes 95% less energy to produce a quantity of hydrogen than water electrolysis. This however, does not account for kinetics of the reaction.

The most widely accepted mechanism of ammonia oxidation is 1) the adsorption of ammonia on to Pt surfaces, 2) dehydrogenation of ammonia into various adsorbed intermediates (N, NH, NH₂), 3) reaction of the intermediates to form N₂H_{2,ad}, N₂H_{3,ad} and N₂H_{4,ad} which then react with OH⁻ to produce nitrogen [37]. The reaction of N₂H_{2,ad} is considered the rate determining step. Vidal-Iglesias et al [38-39] conducted differential Electrochemical Mass Spectrometry (DEMS) studies on ammonia oxidation and suggested also the presence of an azide intermediate species (N₃⁻) at certain potentials. Of the various adsorbed intermediates, NH and NH₂ are active, however, N remains adsorbed (N_{ad}) and acts as a poison.

Although ammonia electrolysis is thermodynamically favorable, kinetics are slow. In practice, high overpotentials are required to drive the ammonia oxidation reaction, and deactivation of the Pt catalyst is observed at high current densities [40-41]. With Pt, N_{ad} is only formed at very high potentials, thus making Pt the best choice of catalyst for electro-oxidation of ammonia. Alloys of Pt have been found effective as catalysts for ammonia oxidation, with the other metals in the alloy chosen for their ability to dehydrogenate ammonia. Endo et al [42] studied combined catalysts of Pt with other metals including Ir, Cu, Ni, and Ru. They concluded that only Ru and Ir can improve the catalytic properties of Pt. In another study, an alloy of bulk Pt with bulk Ir was tested, and the performance was found to be better than Pt alone, however oxidation current densities were still less than 1 mA/cm² [43]. De Voys et al [40] studied ammonia oxidation and intermediates on various polycrystalline catalyst surfaces – Pt, Pd, Rh, Ru, Ir, Cu, Ag, and Au. They concluded that only Pt and Ir combine a good capability to dehydrogenate ammonia with a low affinity to produce N_{ad}. In another study, a Pt-Ir powder mixture (50 wt.%) impregnated in Teflon and painted on a platinum screen was found to provide much lower overpotentials for the oxidation of ammonia than platinum black [44]. However, in these studies, a very high

loading of precious metal catalysts was used (up to 51 mg/cm²) rendering them uneconomical for fuel cell use.

Botte et al [35] studied the use of Pt-Ru alloys for ammonia oxidation catalysts. Individually, Pt and Ru resulted in fast dehydrogenation of ammonia at low potentials which resulted in fast deactivation of the catalyst. However, when combined, the Pt allowed for a significant rate of recombination of adsorbed nitrogen. A low loading of Ru prevented the fast ammonia dehydrogenation from prevailing over the nitrogen recombination step. They reported that catalyst preparation using co-electrodeposition allows for a low loading of noble metals (~2.5 mg/cm²).

In another study, they evaluated the electrolysis of ammonia on a high surface area Raney Nickel substrate plated with Pt and Rh [45]. The electrodes were characterized by scanning electron microscopy, energy dispersive X-ray spectroscopy, and X-ray photoelectron spectroscopy. All tested electrodes demonstrated that Rh produced a synergistic effect when paired with Pt as a catalyst for ammonia electro-oxidation. Hydrogen was successfully produced from a 1M NH₃/5M KOH solution at 14.54 Wh/g H₂ at a current density of 2.5 mA/cm² by an anode containing 1 mg/cm² Rh and 10 mg/cm² Pt at ambient temperature and pressure. When the Pt loading was reduced to 5 mg/cm², the required energy for electrolysis was 16.83 Wh/g of H₂. They did not report results when Pt alone is used as catalyst. Their results indicated that rhodium can increase the kinetics of the electrolysis reaction while allowing a reduced loading of precious catalysts. Their XPS results indicated that 1 mg/cm² is the optimum loading of Rh, since it maximized the proportion of the noble metal coverage to exposed substrate metal. Nevertheless, the energy required to produce hydrogen is nearly 10 times higher than the theoretical thermodynamic value.

In a follow up study, they considered the use of carbon fiber substrate electrodes instead of Raney Nickel [46]. An observed decrease in current density with Raney Nickel at polarization potentials indicated that blockage of active sites by OH⁻ occurred. This blockage was possibly due to non-uniform coverage of the substrate. It resulted in a reduced surface area of the active catalyst. It was proposed that OH⁻ competes with NH₃ for adsorption on to the Pt surface, thereby decreasing the number of available sites for electrolysis. Rh added to Pt has been shown to solve this problem by reducing the number of unused catalyst sites compared with Pt alone. It was also observed that the reactivity of the catalyst decreased over time, indicating that the Ni substrate was not stable. Better results were obtained using carbon fiber electrodes [46-47], which allowed for uniform surface coverage of the noble metal, prevented blockage of active sites, and were light weight compared with Ni. They also obtained promising results using Pt-Ir-Rh and Pt-Ir catalysts on the carbon fiber substrate, which resulted in 91-92% conversion of ammonia to hydrogen at room temperature and low ammonia concentrations, and with electrolysis occurring at current densities up to 25 mA/cm² and a precious metal loading of 5.5 mg/cm². This corresponds to an energy consumption of 18.15 Wh/g of H₂ which is higher than those reported by Cooper and Botte [45], and a hydrogen generation rate of 1.4 mmol/min/g of catalyst.

The previous studies were based on bulk catalysts. Other studies have considered the effects of nano-sized Pt particles, but they found that the oxidation of ammonia was more sensitive

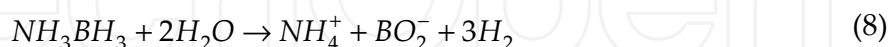
to the structure of Pt particles rather than their size. Vidal-Iglesias et al [48-50] studied ammonia oxidation on stepped electrodes consisting of Pt (1 0 0) terraces and Pt (1 1 1) steps. They used voltammetry, chronoamperometry, and in situ infrared spectrometry to characterize the electrodes and concluded that electrocatalytic activity is increased by a factor of up to 7 when Pt (1 0 0) is used rather than Pt (1 1 1) or Pt (1 1 0) as the preferential orientation of nano-particles. They found that the oxidation was highly structure sensitive and that it took place exclusively on the Pt (1 0 0) sites.

Vidal-Iglesias et al [51] further considered further the effect of adding nano-sized alloys to Pt. Ir, Pd, Rh and Ru were tested. Ru and Pd were found to decrease the oxidation current. In fact, as Ru content increased, the oxidation current decreased. They explained this result by proposing that Pd and Ru decreased the density as well as the dimensions of the Pt (1 0 0) sites. However, Ir and Rh were found to enhance the oxidation current at low potentials. They also studied the effect of particle size and found that 9 nm Pt particles produced better oxidation results than 4 nm particles. This is because the 9 nm particles had a larger number of Pt (1 0 0) sites. They thus concluded that oxidation of ammonia on nano-particles is highly structure sensitive.

Much work has been done in developing catalysts to electrolyze ammonia. Calculations show that the rate of hydrogen generated via electrolysis is in the order of 0.1 to 1 mmol/min/g of catalyst, which is several orders of magnitude lower than what is reported for ammonia decomposition. Also the energy consumption required to produce hydrogen ranges from 14-18 Wh/g. This energy consumption needs to be reduced to 5.4 Wh/g in order to produce H₂ at a realistic cost of US\$2/kg [45]. This means that oxidation overpotentials must be reduced to below 200 mV at much higher current densities than those reported in the literature.

2.4. Hydrogen production from ammonia borane

Products of ammonia have also received some attention in the literature as sources of hydrogen, with most of the studies focusing on ammonia borane (NH₃BH₃) or AB. Ammonia-borane complex has a high material hydrogen content (about 19.6 wt%) with a system-level H₂ energy storage density of about 2.74 kWh/L (versus 2.36 kWh/L for a liquid hydrogen). Hydrogen can be evolved via hydrolysis of AB.



To employ H₂ as a direct fuel supply for PEMFCs a suitable catalyst is needed to accelerate the hydrolysis of AB. Various catalysts with excellent catalytic performance have been developed [52-63]. These include noble metal based catalysts such as Pt, Ru, Rh, Pd, Pt and Au supported on alumina; combinations of Pt with Ir, Ru, Co, Cu, Sn, Au and Ni supported on carbon, Rh(0) nano-clusters [52-57]; and also non-noble metal based catalysts such as Ni and Co on alumina, and Ni and Co nano-particles, Cu/Cu₂O, Poly(N-vinyl-2-pyrrolidone) (PVP) stabilized Ni, Ni-SiO₂ and Fe-Ni alloys [58-63]. Unfortunately, most of the aforementioned catalysts, except for the magnetic Fe-Ni alloy catalyst, are difficult to use repeatedly in solution because they are in a powdery form or are supported weakly on a substrate. The development of catalysts with high durability is thus important for practical use.

Mohajeri et al [64] studied the room temperature hydrolysis of ammonia borane using K_2PtCl_6 and found the reaction rate to be third order (second order with respect to catalyst concentration and first order with respect to AB concentration) with an activation energy of 86.6 kJ/mol. Their average hydrogen generation rate was 590.3 mmol/min/g of catalyst, although this rate varied throughout the test. Good results were also obtained using non-precious metal catalysts. Eom et al [65] considered the effect of an electroless-deposited Co-P/Ni foam catalyst on H_2 generation kinetics in AB solution and investigated the cyclic behavior (durability) of the catalyst. The activation energy for the hydrolysis of AB using the Co-P/Ni foam catalyst was calculated to be 48 kJ/mol. Their hydrogen generation rates were an order of magnitude lower than ref [64] at room temperature, but increased with the temperature of the AB solution. After six cycles, the H_2 generation rate dropped to about 70% of the initial values.

Xu et al [62-63,66-67] obtained excellent results for hydrolysis of an ammonia borane / sodium borohydride ($NaBH_4$) mixture in a 5:1 mass ratio. Their various works utilized different non-precious nano-catalysts including Ni/silica, Co/silica nano-spheres, unsupported Co nano-particles and Fe-Ni nano-particles. For unsupported Co and Fe-Ni, they reported extremely high hydrogen generation rates at room temperature. Some hydrogen generation rates they obtained are calculated using data provided in their references. 10 nm unsupported Co nano-particles evolved hydrogen at the rate of 775 mmol/min/g, while $Fe_{0.5}Ni_{0.5}$ generated 178 mmol/min/g, both at room temperature.

Although AB has 19.1 wt% hydrogen content, the gravimetric (mass) hydrogen storage capacity (GHSC) is relatively low. The GHSC of the AB – H_2O system is only 9% when hydrolysis is intended in stoichiometric conditions and even lower with excess H_2O . Practical studies showed that the effective GHSC is typically only 1% [58]. Demirci and Miele [68] considered the effect that storing AB in a solid form and regulating the supply of H_2O would have on the effective GHSC. They used $CoCl_2$ as catalyst, and found that when water was supplied in stoichiometric quantities, an effective GHSC of 7.8% was achieved at 25 °C. They reported the hydrogen generation rate to be 85.9 mmol/min/g of catalyst under these conditions.

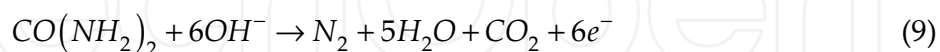
Results in this section show that ammonia borane is extremely promising as a hydrogen source. Hydrolysis of AB has yielded order of magnitude higher rates of hydrogen generation than ammonia decomposition, and it can be done at room temperatures using non-precious metal catalysts. These results are shown in Table 4, which shows significant variations in the performance of the hydrolysis catalysts. For example the hydrogen generation rate using unsupported Co nano-particles is 3 orders of magnitude higher than for Co nano-particles supported on silica. It should also be pointed out that in Ref [62], when the Ni loading increased, the rate of hydrogen generation increased but by an amount less than proportional to the increase in catalyst loading. In other words, as the Ni loading increased, the rate of hydrogen generation per gram of catalyst decreased. Thus there is a lot that is not yet fully understood. The effects of particle size, loading, support as well as other unknown factors need to be investigated in greater detail.

Catalyst	Conditions	Hydrogen Generation Rate (mmol/min/g)	REF
Co-P/ Cu sheet	30 °C	38.7	[65]
Co-P/Ni foam	30 °C	35.8	[65]
	40 °C	69.3	
	50 °C	130.0	
	60 °C	220.1	
K ₂ PtCl ₆ salt	25 °C	590.3	[64]
20-30 nm Ni/Si ₂ O ₃	25 °C	7.0	[62]
15-30 nm Co/ Si ₂ O ₃ nano-spheres	25 °C, NH ₃ BH ₃ / NaBH ₄ mixture	0.7	[66]
10 nm unsupported Co particles	25 °C, NH ₃ BH ₃ / NaBH ₄ mixture	775.0	[67]
Fe _{0.5} Ni _{0.5} nano-particles	25 °C, NH ₃ BH ₃ / NaBH ₄ mixture	178.1	[63]
CoCl ₂	25 °C, NH ₃ BH ₃ / NaBH ₄ mixture	85.9	[68]

Table 4. Performance of Various Catalysts for Ammonia Borane Hydrolysis

2.5. Other means of hydrogen generation from ammonia and ammonia products

Urea is an ammonia product that can be used to generate hydrogen. Urea rich waste water is widely abundant and releases ammonia into the atmosphere when purged into rivers and lakes. Preliminary work has been conducted in urea electrolysis in alkaline media (equations 9,10). Typically a KOH electrolyte is used with a Ni based anode catalyst. One of the problems encountered in the literature is the instability and deactivation of nickel oxide sites during the oxidation of organic compounds [69-70]. Recent research suggested that Rh added to Ni enhances stability, reduce overpotentials and increase current densities by a factor of 200 [71]. Typically KOH is used as the electrolyte, although King and Botte have obtained good results using a polymer gel electrolyte, poly(acrylic acid) (PAA) cross-linked polymer [72]. They found that an electrolyte containing 8M KOH and 15% PAA (by weight) showed a good combination of good conductivity, mechanical strength, and ease of preparation.



Another ammonia product, ammonia hydride was studied by Sifer and Gardner [73] and was proposed for use in military applications requiring low power for long durations. Their study showed that an ammonia hydride system could provide 483 Wh/kg and operate for over 50 hours. This compares well with other batteries used for military applications in terms of energy density.

It is also possible to extract hydrogen by reacting ammonia with metal hydrides such as MgH₂ [74], LiAlH₄ [75] or NaAlH₄ [76]. This can be done at moderate temperatures (75-150

°C) and has been reported to have 2-3 times higher specific energy and energy density than ammonia cracking at 650 °C. However additives are required such as PdCl₂ and PtCl₄ to enhance the rate of hydrogen formation [74]. Paik et al [77] discussed the mechanochemical production of hydrogen from ammonia via milling at room temperature on BaTiO₃ and SrTiO₃ catalysts, however H₂ production rates are relatively low.

3. Direct ammonia fuel cells

When hydrogen is produced from ammonia, there are usually traces of unconverted ammonia and nitrogen oxides in the feed. This is sometimes not amenable for use in fuel cells. The ammonia acts as a poison to Nafion membrane used in PEM fuel cells. For higher temperature fuel cells such as SOFCs, ammonia can be decomposed directly in the fuel cell thus negating the need for an external reactor. This section discusses some research conducted on the direct use of ammonia in fuel cells. It considers PEM fuel cells, SOFCs, alkaline fuel cells, and fuel cells directly utilizing ammonia borane.

3.1. Polymer Electrolyte Membrane (PEM) Fuel Cells Using Ammonia

Ammonia has been proposed for use in PEM fuel cells, however, because of the low temperature of PEM fuel cell operation, internal ammonia decomposition is not thermodynamically favorable. Ammonia must be decomposed externally at higher temperatures, then the hydrogen supplied to the fuel cell. If there is not 100% conversion of ammonia to hydrogen, then there will be trace amounts of ammonia in the hydrogen feed. Unfortunately ammonia has been shown to act as a poison to the Nafion membrane typically used in PEM fuel cells.

Uribe et al [78] studied the effect of ammonia on PEM fuel cells with 0.15-0.2 mg/cm² Pt loading using high frequency resistance (HFR). They exposed the fuel cell intermittently to hydrogen and ammonia at the anode and found that when exposed to 30 ppm ammonia for 1 hour, the performance of the cell degraded, but when it was switched back to neat hydrogen, full recovery of performance was observed after 18 hours. When it was exposed to ammonia for 17 hours, full recovery was not observed within 4 days after switching back to hydrogen. Cyclic voltammetry (CV) did not indicate the presence of any adsorbed species at the anode or the cathode, thus the poisoning mechanism of ammonia on PEM fuel cells was not determined. HFR showed that the cell resistance doubled in 15 hours of ammonia exposure. Soto et al [79] performed a similar study but using higher catalyst loading – 0.45 mg/cm² Pt/Ru at the anode and 0.6 mg/cm² Pt at the cathode. Using the current interrupt technique, they showed that after 10 hours of exposure to 200 ppm ammonia, the cell resistance increased by 35%. As in Ref [78] CV showed no evidence of any adsorbed species at the anode or cathode. They proposed that ammonia affects the anode catalyst layer rather than the cathode catalyst layer, primarily because it is supplied at the anode. In these studies, calculations imply that ohmic losses were not sufficient to explain the loss in fuel cell performance observed.

In another test using 0.45 mg/cm² Pt/Ru at the anode and 0.4 mg/cm² Pt at the cathode with a Nafion membrane, the cell was exposed to 10 ppm ammonia [80]. The cell resistance

gradually increased reaching a steady state value of twice the original value after 24 hours of exposure. During this time, the voltage dropped by 160 mV, of which ohmic losses could only account for 8 mV. The cell recovered to normal operation after 2-4 hours of neat hydrogen. Exposure to 1 ppm of ammonia produced a degradation in performance that was slower than for 30 ppm, but the cell resistance tended to the same steady state value of double the original resistance after more than 1 week of exposure. Using Pt vs Pt/Ru at the anode did not significantly alter the poisoning profile, thus they concluded that it was unlikely to be the anode catalyst layer that was affected. Szymanski et al [81] studied the effect of ammonia on phosphoric acid fuel cells. They found that for a PAFC operating at 191 °C, it was the oxygen reduction reaction at the cathode that was most affected by the presence of ammonia. When 1% of H_3PO_4 was converted to $(\text{NH}_4)\text{H}_2\text{PO}_4$, the cathode activity decreased by 84%.

Halseid et al [80] performed a unique test using a symmetric H_2/H_2 PEM cell – hydrogen supplied at both electrodes. Then one of them was switched to 10 ppm ammonia. They observed that the cell resistance did not decrease when the ammonia supply was stopped, and that a limiting current existed not due to mass transport, but due to a reaction limiting current possibly attributed to the Tafel step in the Tafel-Volmer hydrogen oxidation reaction (HOR) mechanism. They interpreted this to mean that ammonium remains in the membrane phase, confirming the low volatility of ammonium in PFSA ionomers. Performance degradation followed a first order response therefore could not be the result of ammonia adsorption on the carbon of the GDL. Oxidation of ammonia on Pt in acidic solutions to form N_2 or NO_x was also unlikely to be significant at the anode. At high cell potentials, they proposed that a platinum oxide is formed at the catalyst sites, thus reducing the effectiveness of the catalyst. They proposed that ammonium transfers across the PEM membrane within minutes, affecting not only the anode side but the cathode as well. They postulated that ammonium does not adsorb on to the anode catalyst, but shifts the potential of the H_2 adsorption process in Pt solutions, but not H_2 desorption [82]. Ammonium in sulfuric acid (low concentrations 10% NH_4) has been shown to increase the cathode overpotential by up to 100 mV at any given current density. They suggested the possibility of an adsorbed species from the electrochemical oxidation of ammonium that blocks active sites, or the result of a mixed potential at the cathode due to simultaneous oxygen reduction and ammonium oxidation [80].

Hongsirikarn et al [83-84] performed further studies on the effects of ammonia on Nafion, measuring the membrane conductivity in the liquid and gas phases. They prepared their membranes using HCl and NH_4Cl to simulate the desired concentrations of H^+ and NH_4^+ in the membrane. They measured conductivity via a two probe technique using a frequency response analyzer. The room temperature conductivity of Nafion 117 in distilled water decreased almost linearly from 115 mS/cm to 24 mS/cm when NH_3 content increased from 0 to 100%. Ammonia tolerance was also seen to improve with temperature. The effect of ammonia on conductivity was more severe in the gas phase than the aqueous phase because in the gas phase, only small amounts of water vapor were present, and the strong anion sulfonic sites stabilized the ammonium ion in the structure [80]. They also performed tests

exposing Nafion membranes to 5-30 ppm NH₃ gas, similar conditions to operating fuel cells. Conductivity decreased from 30 mS/cm to a steady state value of 2.5 mS/cm over time, with the rate of degradation increasing with ammonia concentration. 30 ppm required roughly 6 hours to reach a steady state poisoning whereas 5 ppm took 36 hours [83].

NH₃ poisoning of PEM fuel cells is a slow process unlike CO poisoning. Recovery is also slow. This is due to the relatively slow diffusion of ammonium in the membrane, and the slow process of ammonium oxidation which results in ammonium sinks (for diffusion). For use in PEM, ammonia must be removed from the fuel stream. Saika et al [85] suggested an ammonia recirculation system that can reduce the ammonia content in the fuel stream from 300 ppm to 0 ppm. This involves dissolving ammonia in water (H₂ and N₂ do not dissolve) and recirculating the ammonia. However, much more work is needed to refine this particular area of research. The alternative is enhancing the catalysts (perhaps the cathode rather than the anode) with other noble metals (perhaps Ir) to enhance ammonium oxidation [80].

To date, no studies have been reported showing the effects of ammonia on polybenzimidazole (PBI) membranes, which are an alternative intermediate temperature polymer electrolyte membrane to Nafion. PBI is normally doped in phosphoric acid and operates up to 200 °C. These conditions are not suitable for internal ammonia decomposition. However it is not known how traces of ammonia in the hydrogen feed would affect the performance of PBI membranes. This remains a subject for future work.

3.2. Direct ammonia solid oxide fuel cell

Ammonia has proven to be problematic for PEM fuel cells involving Nafion since both the conductivity of the membrane and the activity of the catalysts are adversely affected by trace amounts of ammonia in the fuel feed. This requires either 100% conversion of ammonia to hydrogen which is not always guaranteed, or total clean up of ammonia which is not always practical. Various researchers have investigated solid oxide fuel cells for direct ammonia oxidation. In fact ammonia can actually allow for smaller scale operation of SOFCs [86]. Farhad and Hamdullahpur reported a 100 W SOFC system where 1 liter of ammonia can provide nearly 10 hours of sustained power [87].

Ammonia decomposes readily at the high temperatures of SOFCs and has not been shown to act as a poison to the ceramic electrolytes utilized in SOFCs. Research into ammonia SOFCs can be divided into two categories – SOFC-O (oxygen ion conducting electrolytes) and SOFC-H (proton conducting electrolytes). SOFC-O entails an oxygen ion conducting electrolyte, such as yttria stabilized zirconia (YSZ) or samarium doped ceria (SDC), and water formation at the anode. SOFC-H entails a proton conducting ceramic electrolyte such as barium cerate and water formation at the cathode.

3.2.1. Ammonia Fed SOFC-O





The anode and cathode half cell equations for the SOFC-O fuel cell are shown respectively in equations 11 and 12. Pioneering research in this field was conducted by Wojcik et al [88]. They used an SOFC with a YSZ electrolyte at 800 °C with various catalysts – Fe, Ag, and Pt. Their objective was to test the various electrodes (catalysts). Their work raised the possibility of NO formation at the anode according to equation 13.



The objective of the catalyst is to decompose NH₃ to H₂ faster than NO can be produced. Their research has ranked the catalysts in the following order of decreasing performance: Pt > Fe > Ag. They found that with Pt as the catalyst, fuel cells operating with NH₃ showed very little difference in performance to those operating with H₂, indicating that complete decomposition of NH₃ occurs over Pt. They discussed the possibility of using Ni although they did not test it in their fuel cells.

Detailed experimental investigation by Sammes and Boersma [86] have shown that Ni outperformed Ag and Pt in the temperature range 500 – 800 °C, with 90% conversion of ammonia occurring at 800 °C. Choudhary and Goodman [89] suggested that Ni electrodes can produce 5-10 times higher power densities than Ag or Pt. As the temperature increases, the performance of the ammonia fed cell approaches that of the hydrogen fed cell since conversion of ammonia approaches 100%, confirming the findings of Wojcik et al [88]. With the Ni-YSZ/YSZ/Ag (Ni-YSZ anode, YSZ electrolyte and Ag cathode) system at 700 °C, the ammonia cell actually performed better than the hydrogen cell. At 800 °C, a planar SOFC showed a peak power density of 75 mW/cm² (using a 0.4 mm thick electrolyte) while a tubular SOFC showed a peak power density of 10 mW/cm² (using 1 mm thick electrolytes). Fournier et al found that at 800 °C, a peak power density of 60 mW/cm² was achieved [90]. Dekker and Rietveld [91] used an anode supported system – NiO-YSZ/YSZ/LSM at 700 °C and obtained a peak power density of 55 mW/cm². They suggested that the temperature be at least 700 °C for sufficient ammonia conversion.

Most of the early work used electrolyte supported systems, which contained thick electrolytes with high ohmic overpotentials. As a result their peak power densities were in the order of 10 mW/cm². Zhang et al [92] prepared thin electrolytes (15 μm thick) by coating onto the anode substrate by a vacuum assisted dip-coating method using a YSZ slurry. Their anode supported NiO-YSZ tube was prepared by extrusion method. Their results showed a peak power density of 200 mW/cm² at 800 °C with NH₃ as fuel with no NO_x emissions detected. The equivalent peak power density with H₂ as fuel was 202 mW/cm². Ma et al [93] tested anode supported SOFCs based on a YSZ thin film electrolyte (30 μm thick), prepared by dry pressing, which they reported to be a reproducible way of producing thin film electrolytes by controlling the amount of powders used. With liquid ammonia as the fuel, they obtained power densities of 299 and 526 mW/cm² at 750 and 850 °C respectively. These results reveal a high temperature sensitivity. Open circuit voltage (OCV) analysis showed that ammonia oxidation occurs via two stages – cracking of ammonia and oxidation of

hydrogen. The ammonia and hydrogen fueled cells had the same electrolyte resistances, however the ammonia cell had a higher interfacial polarization resistance at temperatures less than 750 °C.

SOFC-O System (anode/electrolyte/cathode)	Electrolyte Thickness (μm)	Temperature	Power Density (mW/cm^2)	REF
Pt-YSZ/YSZ/Ag	200	1000	125	[88]
		900	90	
		800	50	
Ni-YSZ/YSZ/Ag planar Ni-YSZ/YSZ/Ag tubular	400	800	75	[89]
	1000		10	
NiO-YSZ/YSZ/Ag	400	800	60	[90]
NiO-YSZ/YSZ/LSM	150	700	55	[91]
Ni-YSZ/YSZ/YSZ-LSM	30	750	299	[93]
		850	526	
Ni-YSZ/YSZ/YSZ-LSM	15	800	200	[92]
Ni-SDC/SDC/SSC-SDC	50	500	65	[96]
		600	168	
		700	253	
NiO-SDC/SDC/SSC-SDC	24	650	467	[94]
Ni-SDC/SDC/BSCF	10	700	1190	[95]

Table 5. Summary of SOFC-O Peak Power Densities

Another oxygen ion conducting electrolyte tested in the literature is SDC. Liu et al [94] compared liquid methanol, ammonia and hydrogen as fuels in a SOFC with a NiO-SDC anode, a 24 μm SDC electrolyte and a $\text{Sm}_{0.5}\text{Sr}_{0.5}\text{CoO}_3$ (SSC)-SDC cathode. At 650 °C, they obtained peak power densities of 698 mW/cm^2 (methanol), 870 mW/cm^2 (H_2) and 467 mW/cm^2 (NH_3) mW/cm^2 . Meng et al [95] fabricated a 10 μm thick SDC electrolyte using a glycine-nitrate process, with Ni-SDC as the anode and $\text{Ba}_{0.5}\text{Sr}_{0.5}\text{Co}_{0.8}\text{Fe}_{0.2}\text{O}_{3-\delta}$ BSCF as the cathode. A peak power density of 1190 mW/cm^2 was obtained at 700 °C. At this temperature, the performance of a hydrogen fueled cell was 1872 mW/cm^2 . Unlike previous works, they observed marked differences between the ammonia and hydrogen fueled cells at the respective temperatures. Their explanation was that the thermocouple reading was higher than the actual cell temperature because of the endothermic nature of the ammonia decomposition reaction. Nevertheless, their observed power densities were among the highest reported in the literature, primarily because of their thin electrolytes. Also noteworthy is that with the thinner SDC electrolytes, high power densities were observed at lower temperatures. No endurance tests were reported for such thin electrolytes.

With thin electrolytes, the power density of ammonia fed SOFC-O systems has been tremendously improved. At higher temperatures, the conversion of ammonia to hydrogen increases, and as a result, the performance of the ammonia fed system approaches that of the hydrogen fed system. Ni has been shown to be a very active catalyst for the ammonia

decomposition and hydrogen oxidation reactions. However, due to the slow diffusion of oxygen ions through the electrolyte, the anode reaction is the rate limiting step [7]. This allows for the production of NO_x at the anode, although the use of Fe based catalysts can aid in reducing NO_x production. Table 5 summarizes the results of SOFC-O research presented.

3.2.2. Ammonia Fed SOFC-H

SOFC-O requires relatively high temperatures of operation (800-1000 °C), otherwise the conductivity of the YSZ electrolyte suffers, although better peak power densities have been observed with SDC electrolytes than YSZ. At intermediate temperatures (400-600 °C), the conductivity of SOFC-O electrolytes are significantly diminished. This problem can be resolved by utilizing thinner electrolytes which have been achieved, or by using proton conducting electrolytes. At these intermediate temperatures, proton conducting electrolytes such as BaCeO_3 and SrCeO_3 have better ionic conductivity than YSZ, thus making SOFC-H an attractive alternative at these temperatures. Another advantage of using SOFC-H is that since oxygen ions are not conducted through the electrolyte, the chances of producing NO_x are significantly reduced. Some of the common electrolytes proposed include BaCeO_3 and BaZrO_3 , with the former (barium cerate) receiving a lot of attention in the literature. Commonly reported doping materials for barium cerate include gadolinium, praseodymium, and europium. The anode and cathode half cell reactions for the SOFC-H system are shown respectively in equations 14 and 15.



Maffei et al [96-97] published some early work on ammonia fed SOFC-H systems. They used barium cerate doped with gadolinium and praseodymium (BCGP) as the electrolyte, and obtained a peak power density of 35 mW/cm² at 700 °C. This was essentially the same peak power density observed when hydrogen was used as the fuel. It should be noted that their electrolyte was 1.3 mm thick. Gas chromatography analysis showed no NO_x emission. Stability was observed for 100 hours of operation. With a barium cerate doped with gadolinium (BCG) electrolyte, the peak power density was 25 mW/cm². In a subsequent publication [98], they reported barium cerate doped with europium (BCE) as the electrolyte. The BCE powders prepared by conventional solid state synthesis and the final electrolytes pressed to 1 mm thickness. Pt was used as the electrodes. The IV curves showed very little electrode polarization implying that most of the voltage drops were due to ohmic losses in electrolyte. The OCV was less than 0.7 V due to significant electronic conduction in the electrolyte. At 700 °C, the peak power densities observed were 32 mW/cm² for the NH_3 cell and 38 mW/cm² for the H_2 cell. They attributed this difference to the reduced partial pressure of hydrogen due to nitrogen formation in the NH_3 fed cell. Sustained operation was observed for over 200 hours. In yet another publication [99], they used a novel cermet anode consisting of Ni, europium doped barium cerate, a mixed ionic and electronic solid anode (BCE-Ni), and a BCGP electrolyte (1 mm thick). The BCGP and BCE components

were fabricated using conventional solid state synthesis techniques. They found the BCE-Ni anode to be superior to the Pt anode in that a mere 1% weight composition of Ni was observed to completely decompose ammonia at 650 °C. Peak power densities at 600 °C for the NH₃ fed system were 28 mW/cm² using the NiO anode compared to 23 mW/cm² using Pt. Sustained operation was observed for over 500 hours at 450 °C. Thus they obtained sustained performance in their works, but low power densities, primarily because of the extremely thick electrolytes used in their tests.

Other researchers were able to produce thinner proton conducting electrolytes to obtain much higher current densities. Ma et al [100] used BCG electrolytes and obtained a peak power density of 355 mW/cm² at 700 °C. they observed OCV values of 1.102 V at 600 °C and 0.985 V at 700 °C. These values were consistent with theoretical predictions indicating that complete decomposition of ammonia took place. Zhang et al [101] also used BCG electrolytes dry pressed over a Ce_{0.8}Gd_{0.2}O_{1.9} (CGO)-Ni anode substrate, and obtained peak power densities of 147 mW/cm² at 600 °C. Their OCV was 1.12 V at 600 °C and 1.10 V at 650 °C. These values are slightly lower than those for hydrogen fed cell because of the reduced partial pressure of the hydrogen due to nitrogen.

Ma et al [93,102] used 50 µm thin film BCG electrolytes with Ni-BCG anode and LSC-BCG cathode, and obtained peak power density of 355 mW/cm² and an OCV of 0.975 V at 700 °C. Gas chromatography showed that the partial pressure of NO was in the order of 10⁻¹² atm. Lin et al [103] had similar observations with a 35 µm BaZr_{0.1}Ce_{0.7}Y_{0.2}O_{3-δ} (BZCY) electrolyte with BZCY/Ni anode and Ba_{0.5}Sr_{0.5}Co_{0.8}Fe_{0.2}O_{3-δ} (BSCF) cathode. Both BZCY and BSCF oxides were synthesized by a combined ethylenediaminetetraacetic acid (EDTA)-citrate complexing sol-gel process. Their peak power densities were 420 and 135 mW/cm² at 700 and 450 °C respectively. At 450 °C, the OCV was 0.98 V with ammonia compared to 1.1 V with hydrogen, the difference being attributed to reduced partial pressure. Based on impedance tests, they concluded that the actual operating temperature of the reaction may be lower (by about 35-60 °C) because of the endothermic nature of the reaction.

SOFC-H System (anode/electrolyte/cathode)	Electrolyte Thickness (µm)	Temperature	Power Density (mW/cm ²)	REF
Pt/BCGP/Pt	1300	700	35	[96]
Pt/BCG/Pt			25	[97]
Pt/BCE/Pt	1000	700	32	[98]
Ni-BCE/BCGP/Pt	1000	600	23	[99]
Ni-BCG/BCG/LSCO	50	700	355	[100]
Ni-BZCY/BZCY/BSCF	35	450	135	[103]
		700	420	
Ni-CGO/BCG/BSCF	30	600	147	[101]
NiO-BCNO/BCNO/LSCO	20	700	315	[104]

Table 6. Summary of SOFC-H Peak Power Densities

Zhang and Yang [101] were able to further reduce the electrolyte thickness to 30 μm based on a CGO-Ni/BCG/BSCF system and obtained a peak power density of 147 mW/cm^2 at 600 $^\circ\text{C}$. The thinnest proton conducting electrolyte reported was a 20 μm $\text{BaCe}_{0.9}\text{Nd}_{0.1}\text{O}_{3-\delta}$ (BCNO) electrolyte fabricated with a suspension spray method, with a NiO-BCNO anode and a $\text{La}_{0.5}\text{Sr}_{0.5}\text{CoO}_{3-\delta}$ (LSCO)-BCNO cathode [104]. Their peak power density was only 315 mW/cm^2 however. They attributed this lower than expected value to the dense anode layer which resulted in incomplete reduction of NiO into Ni, thereby reducing the activity of the anode catalyst. Tests with a less dense anode were not reported. Table 6 summarizes the results of SOFC-H systems reported.

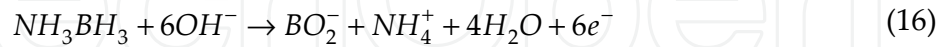
A significant advantage of direct ammonia SOFCs is that non-precious metal catalysts can be used. Nickel has been shown to be the most effective anode catalyst for both SOFC-O and SOFC-H – for both ammonia decomposition and hydrogen oxidation. This is critical for cost reduction. Perhaps SOFCs hold the best prospects for direct ammonia use in fuel cells. Thin electrolytes have been achieved with both SOFC-O and SOFC-H and both have reported high power densities. Most importantly, the performance of the SOFC has not been reported to be significantly diminished using ammonia instead of hydrogen as the fuel. There is no clear consensus on which of the two SOFC types is better. Although, some studies have reported concerns about NO_x formation at the anode of SOFC-O, in practice this has not been observed. NO formation is more likely in SOFC-O at high temperatures and high current densities when both the ammonia decomposition rate and the oxygen ion flow rate are high. However, in one study, NO was not detected up to 800 $^\circ\text{C}$ [102]. With anode supported SOFC-O systems (thick anodes and thin electrolytes), gas chromatography studies have shown that NH_3 completely decomposes by the Ni catalyst long before it reaches the triple phase boundary (TPB) [92].

3.3. Other Types of Ammonia Fuel Cells

Anhydrous ammonia has been proposed for use in alkaline fuel cells [105]. Aqueous alkaline electrolytes are tolerant to ammonia, unlike Nafion used in PEM fuel cells [10,20,34,106]. In a test cell, an AFC was run on ammonia for over 100 hours without any signs of poisoning [107]. However, at the low temperatures in which AFCs operate, ammonia will not readily release hydrogen atoms, therefore a separate external reformer is required [105]. Ganely [108] developed a test cell using a eutectic mix of NaOH and KOH fueled with pure ammonia and compressed air. The peak power density observed was only 40 mW/cm^2 at 450 $^\circ\text{C}$. The electrodes were Ni tubes dipped into the molten electrolyte. One problem observed during the operation of the cell is that at the cathode, Ni oxidized to NiO and suffered reduced conductivity. They solved the problem by pretreating the Ni with 3M LiOH solution at 100 $^\circ\text{C}$ for 24 h while maintaining an anodic current of 1 mA/cm^2 . The Nickel was thermally and electrochemically converted into a hydrated Nickel oxide, which was then electrochemically oxidized and lithiated by cationic exchange to produce LiNiO_2 . This lithiated nickel was more stable and did not polarize during a 2-4 hour test. Nevertheless, the liquid electrolyte system suffers from high ohmic losses due to large electrode separation compared with solid state technology. Also the active catalyst sites are reduced due to the bulk nature of the electrodes. This problem is inherent to AFCs. Another

potential problem with AFCs is that they require air that is free of CO₂, because of an unfavorable reaction between KOH and CO₂ [109].

Ammonia borane has already been discussed as a hydrogen source. However, there has been preliminary work suggesting that it can be utilized directly in fuel cells. This way, a greater reversible potential (1.616 V at 25 °C) can be achieved and thus greater power if it is used directly in fuel cells [110]. The anode and cathode half cell reactions are shown respectively in equations 16 and 17.



In a test cell using a Nafion 117 membrane with Vulcan XC-72 30% Pt catalyst (0.15 mg/cm² loading) and carbon cloth electrodes, a peak power density of 14 mW/cm² was achieved at room temperature [110]. However, in the test cell, it was noticed that hydrogen gas was evolved at the anode indicating that hydrolysis of AB took place. The authors suggested that this could be inhibited by using thorium as an additive. Alternatively increasing the pH could also be used to avoid hydrolysis. In a follow up work, the Nafion membrane was replaced by a 28 μm thick anion exchange membrane from Tokuyama Corp. This time, peak power densities of 110 mW/cm² and 40 mW/cm² were achieved at 45 °C and 25 °C respectively. They also were able to run the fuel cell at 50 mA/cm² and 120 mA/cm² for over 20 hours without noticeable degradation in performance. However, energy dispersive X-ray spectroscopy (EDX) measurements showed that AB migrated across the anion exchange membrane and was directly oxidized at the cathode, thus greatly reducing the cell performance at higher current densities [111]. Kiran et al [112] tested a AB fuel cell using a TiC anode, Pt/C cathode with a Nafion 117 membrane, and obtained a peak power density of 110 mW/cm², 85 mW/cm² and 45 mW/cm² at 80 °C, 60 °C and 25 °C. respectively. This work allowed for the use of a non-precious catalyst, however the performance of the cell at 80 °C was not comparable to Ref [111].

Based on the half cell reactions, a significant amount of hydrogen is not extracted from ammonia borane. Zhang et al [111] suggests that BO₂⁻ can be reverted to BH₄⁻ through a reaction with a saline hydride (MgH). Then it can be converted back to NH₃BH₃ using a diethyl ether at room temperature and recycled. However, this just adds to the overall cost of the system. Another major drawback to ammonia borane fuel cells is that ammonium is produced in the anode reaction and this has already proven to be problematic for Nafion membranes. Based on present research, ammonia borane is more effective as a hydrogen source via hydrolysis than as a direct fuel in fuel cells. Much more work is needed to develop this technology.

4. Modeling and simulation of ammonia fed fuel cells

Research into ammonia fuel cells is relatively new and most of the work reported in the literature has been experimental. There have been a few works devoted to modeling of ammonia fuel cells, however this remains a relatively underdeveloped field. Mathematical

or computational modeling is useful in that it can help attain information on the fuel cell that cannot be measure in situ. Most of the models reported thus far have been thermo-electrical models, with very few reporting comprehensive CFD type modeling. All of these models use parameters reported in the experimental literature.

Ni et al [113] published a thermodynamic model comparing the theoretical performance of SOFC-O and SOFC-H. Their computations showed that SOFC-H had a higher equilibrium potential (1000 vs 850 mV) and higher efficiency (72 vs 61 %) than SOFC-O at 800 °C. This assumed 80% fuel utilization and 20% oxygen utilization, 100% conversion of ammonia, and no formation of NO_x. Efficiency was defined as the ratio of electrical work to the lower heating value (LHV) of ammonia. The efficiency of both fuel cells decreased with temperature because of decreasing reversible potential, however the SOFC-H had an 11% higher efficiency. The reason for the better performance of SOFC-H is that water is not produced at the anode and therefore does not dilute the hydrogen. This model dealt primarily with thermodynamic equilibrium or reversible conditions.

This was followed by a 1D electrical model of a SOFC-H comparing the performance with NH₃ and H₂ as fuel [114]. This model incorporated the Nernst equation, Butler-Volmer equation, ohm's law, and the dusty gas model to determine partial pressures at the electrode/electrolyte interface, with the finite difference method used to solve the system of differential equations. Their results showed that the NH₃ fed cell always maintained a lower potential than the H₂ fed cell. These differences were insignificant for electrolyte supported systems (thick electrolytes), however with anode supported systems (thin electrolytes), the differences became pronounced. N₂ dilution of H₂ was cited as the reason for this observation. At 800 °C, their peak power densities for the SOFC-H / NH₃ system were 68, 440 and 820 mW/cm² respectively for 500, 50 and 10 μm electrolyte thicknesses. In another 1D electrical model, the same authors compared the effect of electrolyte type on NH₃ fed SOFC systems, i.e. SOFC-O vs SOFC-H [115]. Surprisingly they found that under operating conditions (non-equilibrium), the potential of the SOFC-H was lower than that of the SOFC-O especially at higher current densities (respective peak power densities at 800 °C for a 50 μm electrolyte thicknesses were 360 and 420 mW/cm²). This result is not consistent with Ma et al [102], who experimentally compared both systems at 700 °C and found their SOFC-H to have higher power densities than their SOFC-O (355 vs 252 mW/cm², both with 50 μm electrolytes). It is possible that as temperature increases, the SOFC-O performance improves compared to the SOFC-H. It is also possible that Ref [115] used a higher electrolyte resistance for the SOFC-H than those reported in the literature since the results of a model depend heavily on the parameters inputted to the model. They also noted that the SOFC-H had a higher anode concentration overpotential than the SOFC-O but a lower cathode concentration overpotential. It appears that the formation of water increases the concentration overpotential at the electrode where it is formed (anode for SOFC-O and cathode for SOFC-H). Dincer et al [116] performed a similar study and confirmed this finding. However, unlike Ref [115], they found that the SOFC-H outperformed the SOFC-O in both open and closed circuit conditions. Respective peak power densities at 800 °C for 30 μm electrolytes were 700 and 590 mW/cm². It should be noted that Ref [116] used a lower

electrolyte resistance for the SOFC-H than Ref [115], which may account for their contradicting conclusions.

Ni et al [117] published an improved electrical model. The previous models assumed complete decomposition of ammonia, which is not realistic at lower temperatures utilized in SOFC-H. This work accounted for reactive transport of ammonia through the porous anode utilizing correlations reported by Chellappa et al [34], consistent with Ni/Al₂O₃ anode catalysts. Simulations showed that at 800 °C, complete conversion of ammonia to hydrogen occurred in the outer 10% of the anode. At 600 °C, ammonia permeated through 60% of the anode, but decomposed fully. At 400-500 °C however, only 10-40% conversion of ammonia was predicted. They thus recommended that SOFC-H be operated above 600 °C to avoid unconverted ammonia. One weakness of this work is that it did not compare the fuel cell performance with the previous models which assumed complete conversion of ammonia at the intermediate temperatures. This would have allowed a quantification of the effect of unconverted ammonia. The model also did not account for the inhibition effect of hydrogen on ammonia decomposition at the lower temperatures which were reported in the experimental literature (Section 2.2).

Ni et al [118] reported the first CFD based model of ammonia fuel cells. They developed a 2D thermo-electric model that combines a thermodynamic model, an electrochemical model, a chemical model for ammonia decomposition, and a CFD model for heat and mass transfer. This work focused on a planar anode supported SOFC-O based on a Ni-YSZ anode supplied with gases at 600 °C. Results demonstrated that high temperature gradients existed inside the cell – decreasing by up to 100 °C over 5 mm of channel length in some cases. High temperatures occurred near the anode and cathode inlets, but decreased because of the endothermic nature of the ammonia decomposition reaction. The fact that the rate of decomposition increases with temperature exacerbates the thermal gradients. Increasing the current density (decreasing cell potential from 0.8 to 0.3 V) decreased the temperature variations slightly, but not significantly. Increasing the flow velocity also was not shown to be effective in reducing the temperature variation. It was observed that increasing flow velocity by a factor of 10 resulted in a decrease in current density and Nernst potential, thus decreased the heat generation by the electrochemical reactions. This effect was more significant than the increased convection associated with the higher flow rates. The temperature variation actually increased when the flow velocity increased. Decreasing the flow rate, however, decreased the temperature variation to 30-40 °C (between inlet and outlet). They also observed a “cold spot” upstream in the electrolyte, which was approximately 67 °C colder than the inlet temperatures. This observation is consistent with what has been reported in some experimental works [95,103]. This simulation was based on parallel flow operation. No simulation was shown for counter flow operation or for tubular SOFCs with injection tubes, which may help to better distribute the temperature within the fuel cell.

Dincer et al [119] performed an exergy analysis on a combined heat and power system (CHP) with energy storage and heat recovery for vehicular application. The CHP entails an ammonia fed SOFC-H, a microturbine, a compressor, three compact heat exchangers, and a heat recovery unit. Their proposed system used ammonia (stored at 10 bar) and exiting the

compressor at 600 °C before entering the fuel cell. They found that the system efficiency ranged from 60-90 % while energy efficiency ranged from 40-60 %. The rate of entropy generation decreased by 25% for every 100 °C increase in operating temperature. Exergy efficiency increased with current density for both the SOFC and the CHP system. As temperature increased, they observed that energy efficiency decreased while exergy efficiency increased. The authors recommended that the SOFC be operated with an exhaust temperature between 1200 and 1300 °C. It is questionable however whether such high temperatures are appropriate for vehicular applications.

Other works have focused on numerical simulation of the decomposition reactor [120-122]. Chein et al [123] theoretically and numerically predict H₂ generation over packed beds of Ni-Pt/Al₂O₃ particles using a chemical reaction model to account for varying rates of ammonia decomposition. Their results indicated that the porosity and permeability of the packed bed did not significantly affect the performance of the reactor, at least for the range of values investigated, and that their results gave the same predictions as a 1D plug flow model. They recommended low flow rates of ammonia to increase the residence time in the reactor, thus allowing for higher conversion efficiencies to be attained at lower temperatures. However, one major assumption in their model is that of an isothermal reactor. Ni [118] has shown that there are significant temperature variations as a result of the endothermic nature of the ammonia decomposition reaction. It is also possible that the model reported in Ref [123] was too simplistic, and did not account for the effects of intermediate species, which may depend on porosity and permeability.

Alagharu et al [124] modeled an ammonia decomposition reactor for a 100 W PEM fuel cell. It was shown that operating the reactor adiabatically results in a sharp decrease in temperature due to endothermic reaction, which resulted in low conversion rates of ammonia. For this reason, the reactor was heated electrically to provide heat for the endothermic reactions. It was observed that when the reactor was operated non-adiabatically, it was possible to get over 99.5% conversion of ammonia. In this simulation, fuel entered the reactor at 520 °C, decreasing to 480 °C within the first 5% of the reactor, then exiting at nearly 600 °C. They proposed operating conditions where ammonia is supplied to the reactor at 0.9 mmol/s, supplying a power of 142 W to a stack of 20 PEM fuel cells, of which 42 W is used to heat the reactor.

Thus far, modeling of ammonia fuel cells is a new field of research. The present models account for direct internal ammonia decomposition in the fuel cell anode, however, all the models have reported SOFC performance at elevated temperatures (600-800 °C). It is also possible to operate SOFC-H at lower temperatures (400-500 °C), however no model has as yet taken into account the effect of hydrogen inhibition on the rate of ammonia decomposition that has been reported at these temperatures (section 2.2). Fuel cell models should also propose strategies for dealing with temperature drops inside the fuel cell due to the endothermic nature of ammonia decomposition. Reduced temperature adversely affects the performance of the cell, while high thermal gradients adversely affect its longevity. Future models must also consider the effect of the nano and micro structure on fuel cell performance – the effect of catalyst particle size, particle loading with the supports, and

support conductivity. Also no work has as yet simulated the ammonia poisoning effect in PEM fuel cells or the behavior of direct ammonia borane fuel cells. These are all subjects for future work.

5. Conclusions

Ammonia has been shown to be a cost effective means of hydrogen storage for fuel cells. Its energy cost based on high heating value is less than hydrogen, natural gas, propane and methanol. Also the life cycle cost of power is estimated to be lower for ammonia than for methanol or hydrogen. Studies have shown that for small scale systems, hydrogen generation from ammonia cracking is lower in cost than natural gas reformation and water electrolysis. Ammonia has the added advantage of being widely produced globally and possessing a transport and storage infrastructure that already exists – a significant advantage over hydrogen. Thus ammonia has proven to be a cost effective alternative to hydrogen for fuel cells.

Hydrogen generation from ammonia and ammonia products has been widely studied. Much research has been devoted to developing suitable catalysts for ammonia decomposition. It is widely agreed that Ru is the best catalyst for decomposition at 400 °C, while Ni based catalysts perform comparably at 600 °C. Studies have shown that carbon nanotubes function very effectively as a support for Ru. Treating the support with potassium based alkalis has resulted in a 5-fold increase in catalyst activity. Ni has the advantage of being non-precious. Although the decomposition rate (measured per gram of catalyst) is lower for Ni than Ru at a given temperature, higher loading of Ni is permissible because of its lower cost. Ni also allows for the use of nano-sized particles, which have shown to produce decomposition rates comparable to Ru. There is much scope for improving the low temperature performance of Ni through the use of nano-technology. The mechanism for ammonia decomposition has been widely studied over Ru based catalysts, however there is a general lack of research studying the corresponding mechanism over Ni. Such studies have resulted in the development of supports and promoters that optimize the performance of Ru as a decomposition catalyst. Various supports for Ni have been investigated (silica, alumina, SBA) without any clear consensus on which is optimal. The performance of Ni can be optimized by studying the reaction mechanism and investigating the effect of various promoters.

The hydrolysis of ammonia borane has also been shown to be a very effective means of hydrogen generation, with hydrogen generation rates (per gram of catalyst) being reported to be an order of magnitude higher than for ammonia decomposition. Further, hydrolysis of ammonia borane can occur at room temperature. Excellent results have been obtained with Pt as well as Co, Ni and Fe based catalysts. However, the results reported in the literature vary greatly. For example, two studies by the same research group of ammonia borane hydrolysis using Co based nano-catalysts have produced room temperature hydrogen generation rates that differ by three orders of magnitude. It is not yet fully understood what are the optimal particle size, loading and support required to produce effective hydrolysis

catalysts. Much more work is needed to refine this technology, although it holds tremendous potential for low temperature fuel cells.

Ammonia has also been considered for direct use in fuel cells. PEM fuel cells are adversely affected by ammonia because of reduced conductivity of Nafion and decreased activity of the catalyst layers (especially the cathode). Alkaline fuel cells are unaffected by ammonia but are unlikely to be commercially pursued because of the inherently poor performance associated with non-solid state technologies. High power densities have been reported for SOFCs (100-1000 mW/cm² for both proton conducting and oxygen ion conducting electrolytes). Ammonia is internally decomposed at the high operating temperatures of SOFCs. Early works have focused on Pt based catalysts, however later works have achieved comparable results using Ni based catalysts. The general consensus among researchers is that at higher temperatures, the performance of ammonia fed SOFCs approach that of hydrogen fed SOFCs, differing only due to nitrogen dilution at the anode. However, the works reported suggest that temperatures over 700 °C are required for SOFCs to produce sufficiently high power densities. At lower temperatures, the ammonia to hydrogen conversion efficiency decreases with Ni based catalysts. It is possible and desirable to operate an SOFC-H at temperatures as low as 400 °C, however good performance at such low temperatures has not been reported. The use of nano-sized Ni particles in the SOFC anode has not as yet been reported, but may hold tremendous potential for improving the low temperature performance of SOFC-H. Future work needs to study the preparation and dispersion methods of such catalysts.

There is also much scope for mathematical modeling of ammonia fed SOFCs. So far, few models have been developed, with most of them focusing on thermodynamic considerations. Only one CFD based model has been reported, which revealed that a cold spot exists within the SOFC which reduces its performance. CFD based models can provide strategies for eliminating or reducing the effects of this cold spot. All of the models reported so far have simulated internal ammonia decomposition at relatively high SOFC temperatures (~800 °C). It is desirable to operate the SOFC at much lower temperatures, where the effect of hydrogen inhibition on the decomposition rate has been reported in the experimental literature. No mathematical models have thus far considered this effect. Future models must simulate the behavior of lower temperature SOFCs and the effect of hydrogen inhibition on the ammonia decomposition reaction. They must also consider the effect of catalyst particle size and loading within the support, as well as conductivity of the support on internal ammonia decomposition. Further all of the models focus on SOFCs. Models of the ammonia poisoning effect on PEM electrolytes and catalysts may reveal strategies for reducing this poisoning effect and optimizing the performance of ammonia fed PEM fuel cells. This also remains a subject for future research.

Ammonia can achieve all the benefits of a hydrogen economy with existing infrastructure. Combined with the development of proton conducting SOFC electrolyte technology and Ni based nano-catalyst technology, ammonia allows for smaller scale operation of SOFCs at reduced temperatures (~ 400 °C), which makes it a very attractive power source for small

scale stationary and portable applications. Ammonia may very well be the fuel that makes fuel cell technology commercially viable.

Author details

Denver Cheddie

Center for Energy Studies, University of Trinidad and Tobago, Brechin Castle, Couva, Trinidad and Tobago

6. References

- [1] Christensen CH, Johannessen T, Sorensen RZ, Norskov JK (2006). *Catal. Today* 111:140–144.
- [2] Jensen JO, Vestbo AP, Li Q, Bjerrum NJ (2007). *J. Alloys Compd.* 446-447:723–728.
- [3] Zamfirescu C, Dincer I (2008). *J. Power Sources* 185:459–465.
- [4] Kaye IW, Bloomfield DP (1998). *Conference of Power Source, Cherry Hill*:408–409.
- [5] Yin SF, Xu BQ, Zhou XP, Au CT (2004). *Applied Catalysis A: General* 277:1–9.
- [6] Ni M, Leung MKH, Leung DYC (2009). *Int. J. Energy Res* 33:943–959.
- [7] Lan R, Irvine JTS, Tao S (2012). *Int. J. Hydrogen Energy* 37:1482–1494.
- [8] Lipman T, Shah N (2007). UC Berkeley: UC Berkeley Transportation Sustainability Research Center Retrieved from: <http://escholarshiporg/uc/item/7z69v4wp>.
- [9] Papapolymerou G, Bontozoglou V, Mol J. (1997). *Catal. A: Chem.* 120:165.
- [10] Choudhary TV, Svadinaragana C, Goodman DW (2001). *Catal. Lett.* 72:197.
- [11] Liu HC, Wang H, Shen JH, Sun Y, Liu ZM (2008). *Applied Catalysis A: General* 337:138–147.
- [12] Li XK, Ji WJ, Zhao J, Wang SJ, Au CT (2005). *J. Catal.* 236:181–189.
- [13] Zhang J, Xu HY, Jin XL, Ge QJ, Li WZ (2005). *Appl. Catal. A* 290:87–96.
- [14] ZhEng. WQ, Zhang J, Ge QJ, Xu HY, Li WZ (2008). *Applied Catalysis B: Env* 80:98.
- [15] Plana C, Armenise S, Monzón A, García-Bordejé E (2010). *Journal of Catalysis* 275:228–235.
- [16] Yin SF, Zhang QH, Xu BQ, Zhu WX, Ng CF, Au CT (2004). *J. Catal.* 224:384.
- [17] Yin SF, Xu BQ, Wang SJ, Ng CF, Au CT (2004). *Catal. Lett.* 96:113.
- [18] Wang SJ, Yin SF, Li L, Xu BQ, Ng CF, Au CT (2004). *Appl. Catal. B: Environ* 52:287.
- [19] Bradford MCJ, Fanning PE, Vannice MA (1997). *J. Catalysis* 172:479.
- [20] Ganley JC, Seebauer EG, Masel RI (2004). *J. Power Sources* 137:53.
- [21] Pyrz W, Vijay R, Binz J, Lauterbach J, Buttrey D (2008). *Topics in Catalysis* 50:180.
- [22] Sorensen RZ, Klerke A, Quaade U, Jensen S, Hansen O, Christensen CH (2006). *Catalysis Letters* 112:77.
- [23] Rarog-Pilecka W, Szmigiel D, Kowalczyk Z, Jodzis S, Zielinski J. (2003). *J. Catalysis* 218:465.
- [24] Chen J, Zhu ZH, Wang S, Ma Q, Rudolph V, Lu GQ (2010). *Chem. Eng. J.* 156:404.
- [25] García-García FR, Álvarez-Rodríguez J, Rodríguez-Ramos I, Guerrero-Ruiz A (2010). *Carbon* 48:267.

- [26] Ganley JC, Thomas FS, Seebauer EG, Masel RI (2004). *Catalysis Letters* 96:117.
- [27] Tsai W, Weinberg WH (1987). *J. Phys. Chem.* 91:5307.
- [28] Boudart M, Djega-Mariadassou G (1984). Princeton, NJ:Princeton University Press p 98.
- [29] Löffler DG, Schmidt LD (1976). *J. Catal.* 44:244.
- [30] Egawa C, Nishida T, Naito S, Tamaru K (1984). *J. Soc. Chem. Faraday Trans.* 180:1595.
- [31] Vitvitskii AI, Gaidei TP, Toporkova ME, Kiseleva EM, Melikhov EN (1990). *J. Appl. Chem. USSR* 63:1883.
- [32] Skodra A, Ouzounidou M, Stoukides M (2006). *Solid State Ionics* 177:2217–2220.
- [33] Shustorovich E, Bell AT (1991). *Surf. Sci. Lett.* 259:791.
- [34] Chellappa AS, Fisher CM, Thomson WJ (2002). *Applied Catalysis A: General* 227: 231–240.
- [35] Vitse F, Cooper M, Botte GG (2005). *J. Power Sources* 142:18–26.
- [36] Simons EL, Cairns EJ, Surd DJ (1969). *J. ElectroChem. Soc.* 115:556–561.
- [37] Gerischer H, Mauerer A (1970). *J. Electroanal. Chem.* 25:421.
- [38] Vidal-Iglesias FJ, Solla-Gullon J, Feliu JM, Baltruschat H, Aldaz A (2006). *J. Electroanal. Chem.* 588:331–338.
- [39] Vidal-Iglesias FJ, Solla-Gullon J, Perez JM, Aldaz A (2006). *Electrochem. Comm.* 8:102–106.
- [40] de Vooy ACA, Koper MTM, van Santen RA, van Veen JAR (2001). *J. Electroanal. Chem.* 506:127–137.
- [41] Endo K, Nakamura K, Miura T (2004). *Electrochim. Acta* 49:2503–2509.
- [42] Endo K, Nakamura K, Miura T (2004). *Electrochim. Acta* 49:1635.
- [43] Ge J, Johnson DC (1995). *J. Electrochem. Soc.* 142:3420–3423.
- [44] McKee DW, Scarpellino AJ Jr, Danzig IF, Pak MS (1969). *J. Electrochem. Soc.* 116:562–568.
- [45] Cooper M, Botte GG (2006). *J. Electrochem. Soc.* 153:A1894–A1901.
- [46] Bonnin EP, Biddinger EJ, Botte GG (2008). *J. Power Sources* 182:284–290.
- [47] Boggs BK, Botte GG (2010). *Electrochimica Acta* 55:5287–5293.
- [48] Vidal-Iglesias FJ, Garcia-Araez N, Montiel V, Feliu JM, Aldaz A (2003). *Electrochemistry Communications* 5:22–26.
- [49] Vidal-Iglesias FJ, Solla-Gullon J, Rodriguez P, Herrero E, Montiel V, Feliu JM, Aldaz A (2004). *Electrochemistry Communications* 6:1080–1084.
- [50] Rodriguez P, Herrero E, Solla-Gullon J, Vidal-Iglesias FJ, Aldaz A, Feliu JM (2005). *Electrochimica Acta* 50:4308–4317.
- [51] Vidal-Iglesias FJ, Solla-Gullon J, Montiel V, Feliu JM, Aldaz A (2007). *J. Power Sources* 171:448–456.
- [52] Chandra M, Xu Q (2006). *J. Power Sources* 156:190.
- [53] Chandra M, Xu Q (2007). *J. Power Sources* 168:2135.
- [54] Chandra M, Xu Q (2007). *J. Alloys Compd.* 446:729.
- [55] Yao CF, Zhuang L, Cao YL, Ai XP, Yang HX (2008). *Int. J. Hydrogen Energy* 33:2462.
- [56] Basu S, Brockman A, Gagare P, ZhEng. Y, Ramachandran PV, Delgass WN, Gore JP (2009). *J. Power Sources* 188:238.
- [57] Zahmakiran M, Ozkar S (2009). *Appl. Catal. B: Environ.* 89:104.

- [58] Chandra M, Xu Q (2006). *J. Power Sources* 163:364.
- [59] Kalidindi SB, Indirani M, Jagirdar BR (2008). *Inorg. Chem.* 47:7424.
- [60] Kalidindi SB, Sanyal U, Jagirdar BR (2008). *Phys. Chem. Chem. Phys.* 10:5870.
- [61] Umegaki T, Yan JM, Zhang XB, Shioyama H, Kuriyama N, Xu Q (2009). *Int. J. Hydrogen Energy* 34:3816.
- [62] Umegaki T, Yan JM, Zhang XB, Shioyama H, Kuriyama N, Xu Q (2009). *J. Power Sources* 191:209–216.
- [63] Yan JM, Zhang XB, Han S, Shioyama H, Xu Q (2009). *J. Power Sources* 194:478–481.
- [64] Mohajeri N, Raissi AT, Adebisi O (2007). *J. Power Sources* 167:482–485.
- [65] Eom K, Kim M, Kim R, Nam D, Kwon H (2010). *J. Power Sources* 195:2830–2834.
- [66] Umegaki T, Yan JM, Zhang XB, Shioyama H, Kuriyama N, Xu Q (2010). *J. Power Sources* 195:8209–8214.
- [67] Yan JM, Zhang XB, Han S, Shioyama H, Xu Q (2010). *J. Power Sources* 195:1091–1094.
- [68] Demirci UB, Miele P J. (2010). *Power Sources* 195:4030–4035.
- [69] Schafer HJ (1987). *Top. Curr. Chem.* 142:101–129.
- [70] Vaze A, Sawant S, Pangarkar V (1997). *J. Appl. ElectroChem.* 27:584–588.
- [71] King RL, Botte GG (2011). *J. Power Sources* 196:9579–9584.
- [72] King RL, Botte GG (2011). *J. Power Sources* 196:2773–2778.
- [73] Sifer N, Gardner K (2004). *J. Power Sources* 132:135–138.
- [74] Li L, Hurley JA (2007). *Int. J. Hydrogen Energy* 32:6 – 10.
- [75] Resan M, Hampton MD, Lomness JK, Slattery DK (2005). *Int. J. Hydrogen Energy* 30:1413–6.
- [76] Kircher O, Fichtner M (2005). *J. Alloys Comp.* 404–406:339–42.
- [77] Paik B, Tsubota M, Ichikawa T, Kojima Y (2010). *Chem. Commun.* 46:3982–4.
- [78] Uribe FA, Zawodzinski TA Jr, Gottesfeld S (2002). *J. ElectroChem. Soc.* 149:A293.
- [79] Soto HJ, Lee WK, Van Zee JW, Murthy M (2003). *ElectroChem. Solid-State Lett.* 6:A133.
- [80] Halseid R, Vie PJS, Tunold R (2006). *J. Power Sources* 154:343–350.
- [81] Szymanski ST, Gruver GA, Katz M, Kunz HR (1980). *J. ElectroChem. Soc.* 127:1440.
- [82] Halseid R, Wainright JS, Savinell RF, Tunold R (2007). *J. Electrochemical Soc.* 154:B263.
- [83] Hongsirikarn K, Goodwin JG Jr, Greenway S, Creager S (2010). *J. Power Sources* 195:30–38.
- [84] Hongsirikarn K, Mo X, Goodwin JG Jr (2010). *J. Power Sources* 195:3416–3424.
- [85] Saika T, Nakamura M, Nohara T, Ishimatsu S (2006). *JSME Int. J.* 49:78.
- [86] Sammes NM, Boersma R (2000). *J. Power Sources* 86:98–110.
- [87] Farhad S, Hamdullahpur F, (2010). *J. Power Sources* 195:3084–3090.
- [88] Wojcik A, Middleton H, Damopoulos I, Van herle J. (2003). *J. Power Sources* 118:342–348.
- [89] Choudhary TV, Goodman DW (2002). *Catal. Today* 77:65–78.
- [90] Fournier GGM, Cumming IW, Hellgardt K (2006). *J. Power Sources* 162:198–206.
- [91] Dekker N, Rietveld B (2004). *Proc. 6th European Solid Oxide fuel cell forum: Lucerne, Switzerland.*
- [92] Zhang LM, Cong Y, Yang WS, Lin LW (2007). *Chinese Journal of Catalysis* 28:749–751.
- [93] Ma Q, Ma J, Zhou S, Yan R, Gao J, Meng G (2007). *J. Power Sources* 164:86–89.

- [94] Liu M, PEng. R, Dong D, Gao J, Liu X, MEng. G (2008). *J. Power Sources* 185:188–192.
- [95] Meng G, Jiang C, Ma J, Ma Q, Liu X (2007). *J. Power Sources* 173:189–193.
- [96] Pelletier L, McFarlan A, Maffei N (2005). *J. Power Sources* 145:262–265.
- [97] Maffei N, Pelletier L, Charland JP, McFarlan A (2005). *J. Power Sources* 140:264–267.
- [98] Maffei N, Pelletier L, Charland JP, McFarlan A (2006). *J. Power Sources* 162:165–167.
- [99] Maffei N, Pelletier L, McFarlan A (2008). *J. Power Sources* 175:221–225.
- [100] Ma Q, PEng. R, Lin Y, Gao J, MEng. G (2006). *J. Power Sources* 161:95–98.
- [101] Zhang LM, Yang WS (2008). *J. Power Sources* 179:92–95.
- [102] Ma QL, PEng. RR, Tian LZ, MEng. GY (2006). *Electrochemistry Communications* 8:1791–1795.
- [103] Lin Y, Ran R, Guo Y, Zhou W, Cai R, Wang J, Shao Z (2010). *Int. J. Hydrogen Energy* 35:2637.
- [104] Xie K, Ma QL, Lin B, Jiang YZ, Gao JF, Liu XQ (2007). *J. Power Sources* 170:38–41.
- [105] Kordesch K, Hacker V, Gsellmann J, Cifrain M, Faleschini G, Enzinger P, Fankhauser R, Ortner M, Muhr M, Aronson RR (2000). *J. Power Sources* 86: 162–165.
- [106] Metkemeijer R, Achard P (1994). *J. Power Sources* 49:271–282.
- [107] Hejze T, Besenhard JO, Kordesch K, Cifrain M, Aronsson RR (2008). *J. Power Sources* 176:490–493.
- [108] Ganley JC (2008). *J. Power Sources* 178:44–47.
- [109] Lan R, Tao SW (2010). *ElectroChem. Solid State Lett.* 13:B83e6.
- [110] Zhang XB, Han S, Yan JM, Chandra M, Shioyama H, Yasuda K, Kuriyama N, Kobayashi T, Xu Q (2007). *J. Power Sources* 168:167–171.
- [111] Zhang XB, Yan JM, Han S, Shioyama H, Yasuda K, Kuriyama N Xu Q (2008). *J. Power Sources* 182:515–519.
- [112] Kiran V, Kalidindi SB, Jagirdar BR, Sampath S (2011). *Electrochimica Acta* 56:10493–10499.
- [113] Ni M, Leung DYC, Leung MKH (2008). *J. Power Sources* 183:682–686.
- [114] Ni M, Leung DYC, Leung MKH (2008). *J. Power Sources* 183:687–692.
- [115] Ni M, Leung DYC, Leung MKH (2008). *Int. J. Hydrogen Energy* 33:5765–5772.
- [116] Ishak F, Dincer I, Zamfirescu C (2012). *J. Power Sources* 202:157–165.
- [117] Ni M, Leung DYC, Leung MKH (2008). *J. Power Sources* 185:233–240.
- [118] Ni M (2011). *Int. J. Hydrogen Energy* 36:3153–3166.
- [119] Baniasadi E, Dincer I (2011). *Int. J. Hydrogen Energy* 36:11128–11136.
- [120] Deshmukh SR, Mhadeshwar AB, Vlachos DG (2004). *Ind. Eng. Chem. Res* 43:2986–99.
- [121] Abashar MEE, Al-Sughair YS, Al-Mutaz IS (2002). *Appl. Catal. A*; 236:35–53.
- [122] Waghode AN, Hanspal NS, Shigidi IMTA, Nassehi V, Hellgardt K (2005). *Chem. Eng. Sci.* 60:5862–77.
- [123] Chein RY, Chen YC, Chang CS, Chung JN (2010). *Int. J. Hydrogen Energy* 35:589–597.
- [124] Alagharu V, Palanki S, West N (2010). *J. Power Sources* 195:829–833.